

Selective Creation of Thermal Injury Zones in the Superficial Musculoaponeurotic System Using Intense Ultrasound Therapy

A New Target for Noninvasive Facial Rejuvenation

W. Matthew White, MD; Inder Raj S. Makin, MD, PhD; Peter G. Barthe, PhD; Michael H. Slayton, PhD; Richard E. Gliklich, MD

Objectives: To transcutaneously deliver intense ultrasound (IUS) energy to target the facial superficial musculoaponeurotic system (SMAS), to produce discrete thermal injury zones (TIZs) in the SMAS, and to demonstrate the relative sparing of adjacent nontargeted layers superficial and deep to the SMAS layer.

Methods: In 6 unfixed human cadaveric specimens, the SMAS layer was visualized and targeted using the ultrasound imaging component of the IUS device. Using 2 IUS handpieces, 202 exposure lines were delivered bilaterally in multiple facial regions by varying combinations of power and exposure time (0.5-8.0 J). Tissue was then excised and examined grossly and histologically for evidence of thermal injury using nitroblue tetrazolium chloride viability stain.

Results: Reproducible TIZs were produced selectively in the SMAS at depths of up to 7.8 mm, and sparing of surrounding tissue including the epidermis. Higher energy settings and high-density exposure line pattern produced a greater degree of tissue shrinkage.

Conclusions: In human cadaveric facial tissue, IUS can noninvasively target and selectively produce TIZs of reproducible location, size, and geometry in the SMAS layer. The ability to produce focused thermal collagen denaturation in the SMAS to induce shrinkage and tissue tightening has not been previously reported and has significant implications for aesthetic facial rejuvenation.

Arch Facial Plast Surg. 2007;9:22-29

THE SUPERFICIAL MUSCULOAPONEUROTIC SYSTEM (SMAS) is a continuous fibrous network that envelops the muscles of facial expression and extends superficially to connect with the dermis of the skin.^{1,2} The function of the SMAS is to transmit the activity of the facial mimetic musculature to the facial skin to coordinate facial expression. The SMAS is composed of collagen and elastic fibers in similar proportions to the skin dermis.^{3,4} The SMAS and facial skin exhibit viscoelastic properties, but it has been demonstrated that the SMAS has much greater holding properties and more delayed stress relaxation after a surgical "lifting" procedure.⁵

Several nonsurgical modalities have been developed in an effort to treat facial rhytids (peels, microdermabrasion, and lasers).^{6,7} These modalities have primarily focused on treating the superficial layers of the skin owing to limitations in penetration depth. One of the most effective treatments for facial rhytids has been ablative skin resurfacing

with carbon dioxide or erbium lasers, which creates a sublethal thermal injury in the skin, causing removal of the epidermis and contraction and remodeling of the dermis. Although ablative skin resurfacing has proved efficacious in the treatment of superficial rhytids, its use has been limited by the adverse effects of treating the superficial skin, including prolonged erythema and possible permanent pigmentary changes. For this reason, nonablative skin resurfacing devices (intense pulsed light, light-emitting diode, radiofrequency [RF], Nd:YAG, and pulsed dye lasers) have been designed in an effort to reduce some of the unwanted adverse effects of ablative skin resurfacing.⁸ Although these nonablative skin resurfacing modalities have fewer adverse effects than ablative skin resurfacing, the efficacy is less than desirable. Furthermore, neither modality is designed to specifically address the SMAS layer.

Intense ultrasound (IUS) is an energy modality that can propagate through tissue up to several millimeters. However, for skin tissue when the beam is directed in

Author Affiliations: Division of Facial Plastic and Reconstructive Surgery, Department of Otolaryngology, Massachusetts Eye and Ear Infirmary, and Department of Otolaryngology and Laryngology, Harvard Medical School, Boston (Drs White and Gliklich); and Ulthera Inc, Mesa, Ariz (Drs Makin, Barthe, and Slayton).

a tight focus at a given depth, thermal coagulative necrosis occurs in that focal volume of tissue, leaving the superficial layers unaffected.⁹⁻¹¹ Ultrasound waves induce a vibration in the composite molecules of a given tissue during propagation, and the thermoviscous losses in the medium lead to tissue heating. It has been well established in the literature that IUS fields transcutaneously directed into whole-organ soft tissue can produce coagulative necrosis, resulting primarily from thermal mechanisms.^{9,10} During the past decade, the clinical use of focused IUS has been investigated as a noninvasive surgical tool to treat whole-organ tumors, such as liver, breast, and uterus.

Working in conjunction with the manufacturer (Ulthera Inc, Mesa, Ariz), a novel IUS approach has been developed specifically for treating facial soft tissues and targeting the SMAS. The prototype focuses energy in tissue to produce a 25-mm line of discrete lesions spaced 0.5 to 5.0 mm apart (**Figure 1**). Furthermore, imaging and targeted energy exposure can be accomplished using the same handpiece. Preclinical studies conducted by our group¹¹ using porcine skin, a model with skin structure similar to humans, have demonstrated that the IUS system reliably creates small, well-defined, controllable thermal injury zones (TIZs) in dermal or subdermal soft tissues.

The ability to achieve noninvasive thermal injury and reproducible precise and selective collagen denaturation in the SMAS has not been previously reported, to our knowledge. The potential of this approach to cause selective SMAS contraction might have important implications for treatment of the aging face. We postulate that this device is capable of delivering energy to the deep soft tissue layers of the face, such as the subdermal connective tissues (the SMAS). The objectives of this study are, therefore, to deliver IUS energy to targeted areas of the subcutaneous facial tissue, in particular, the SMAS; to produce discrete lesions from thermal injury in the SMAS; and to demonstrate the relative sparing of adjacent nontargeted layers, such as the epidermis and deeper tissues.

METHODS

Approval for this experiment was obtained from the Massachusetts Eye and Ear Infirmary institutional review board. Six nonfixed, frozen, whole cadaveric head specimens were obtained from a tissue bank supplier (International Biological Inc, Gross Pointe, Mich). The cadavers consisted of 2 males and 4 females aged 49 to 72 years. None of the specimens had evidence of previous facial surgical procedures. The specimens were stored in a freezer and could be identified by a serial number tag.

IUS SYSTEM

The IUS system (Ulthera Inc) is a device designed to target and deliver focused IUS in human tissue. The IUS handpiece contains a transducer that has 2 functioning modes: imaging (which is used to image the region of interest before the therapeutic ultrasound exposures) and treatment (which is the mode that delivers a series of higher-energy ultrasound exposures). In treatment mode, the transducer delivers a series of precise ultrasound pulses along a linear path. The handpiece is designed to mechanically slide in a straight line to deliver a series of ultrasound exposures. For each series of exposures, the following source con-

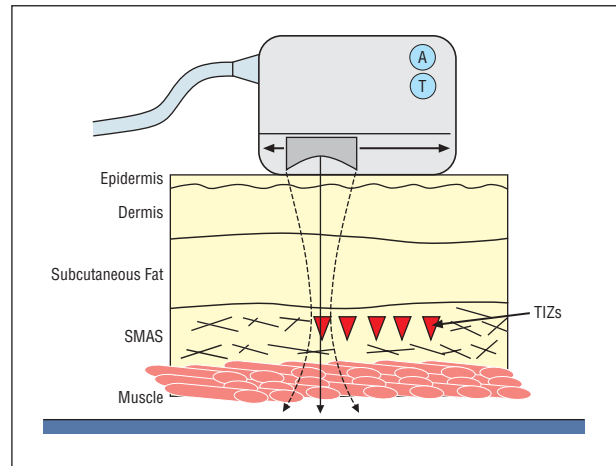


Figure 1. Schematic of intense ultrasound exposures. The intense ultrasound handpiece focuses energy at depths to create thermal injury zones (TIZs) in the superficial musculoaponeurotic system (SMAS) layer. The parabolic transducer slides in the handpiece to create multiple TIZs at a fixed depth in tissue. As an added safety feature, the intense ultrasound device cannot be deployed without first arming the device. This is similar to a laser in the “standby” mode. A indicates arm; T, treat.

ditions can be varied: power output, exposure time, length of exposure line, distance between exposure zones, and time delay after each exposure. In this manner, thermal injury can be produced in selective zones in a straight line at a given depth in the tissue (a 25-mm line of discrete lesions spaced 0.5-5.0 mm apart).

Penetration depth of energy is primarily affected by ultrasound source frequency. The preclinical experiments¹¹ in ex vivo porcine tissues have shown that handpieces with higher ultrasound frequency combined with a shallower focal depth in tissue produce lesions more superficial in tissue, whereas lower-frequency handpieces tend to penetrate deeper in tissues. The results of this study are from handpieces operating at 7.5 and 4.4 MHz, with the focal depth in tissue for each handpiece being 4.5 mm.

IUS EXPOSURE PROCEDURE

Experiments were conducted with the cadaveric specimens at room temperature (20°C) after they had been thawed overnight in a water bath. Multiple facial areas were selected bilaterally: cheek, preauricular area, temple, frontal area, and neck. In the planned treatment area, the skin was tattooed (India ink) to the level of the SMAS using a preconstructed grid (**Figure 2A**). Each microtattoo was placed 10 mm apart in horizontal and vertical lines to create a permanent grid over the proposed treatment area.

Facial areas of treatment were then selected. A range of source conditions was selected and planned for each area. Before each treatment, ultrasound imaging was performed to identify the target tissues. Ultrasound imaging was performed on each planned treatment area, and still images were captured and stored. The superficial and deep skin layers, fat, SMAS, parotid fascia, and parotid gland were discernible during the ultrasound imaging mode.

All the treatments were performed perpendicular to the relaxed skin tension lines of the cadaveric face. The IUS exposure lines were delivered using 2 methods: (1) up to 7 horizontal rows of exposures spaced 10 mm apart at varying energy levels or (2) in a “high-density line” pattern achieved by placing multiple parallel exposure lines (n=15-20) at a fixed energy level 2 to 3 mm apart. Immediately after IUS exposure lines were delivered, the handpiece was left in place, and the axis of

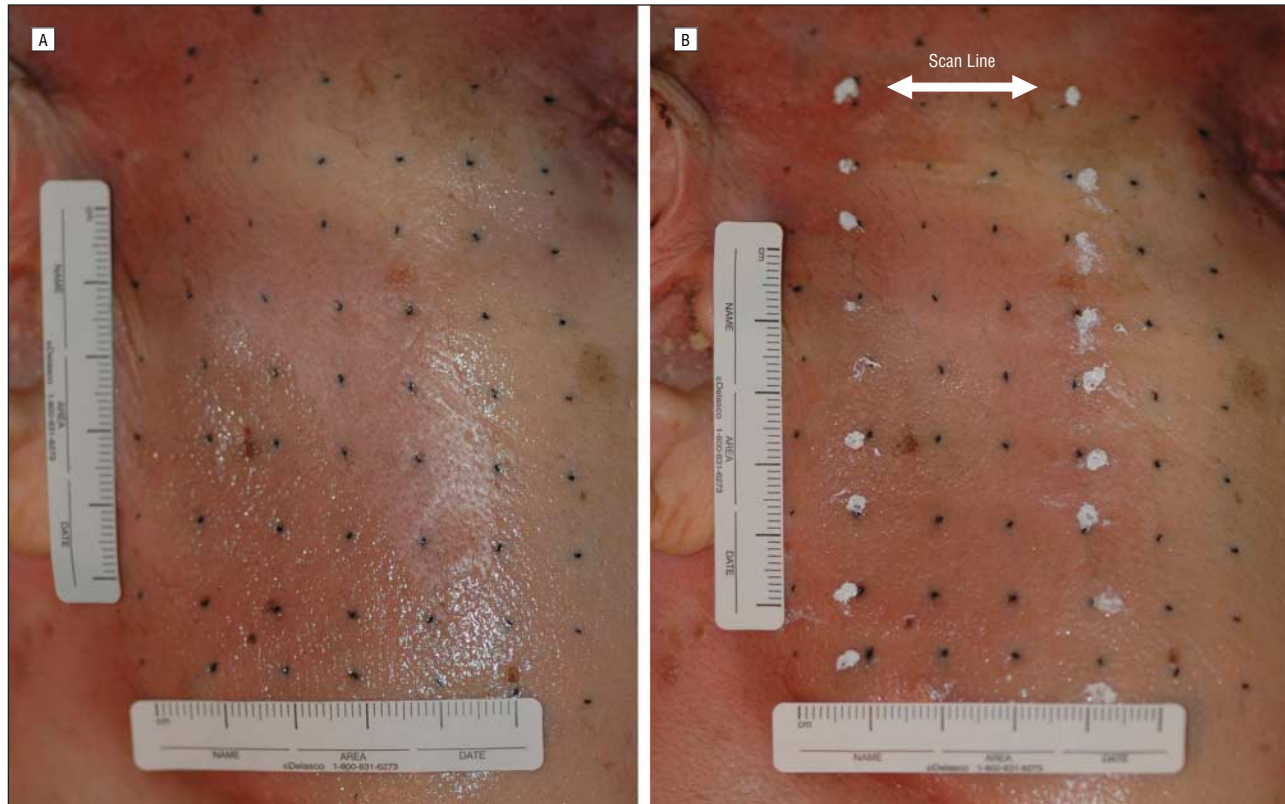


Figure 2. Digital photographs of the intense ultrasound exposure area: right preauricular area. A, Before the exposures, grids were created using India ink tattoos. The intense ultrasound exposures were delivered horizontally along these treatment grids and, therefore, perpendicular to relaxed skin tension lines. B, Immediately after treatment the exposure lines were marked using correction fluid to aid in localizing the lesions.

the exposure line delivered was marked using correction fluid (Wite-Out; Bic Corp, Milford, Conn) (Figure 2B).

After all IUS exposures for a given cadaveric specimen had been completed, each treated facial region was excised en bloc up to the subperiosteal level. The tissue bloc was then placed on an acrylic glass (Plexiglas; Arkema Group, Philadelphia, Pa) tray and kept in a -15°C freezer for approximately 2 hours. Using a surgical blade, fine 1-mm-thick sections were cut perpendicular to the IUS exposure lines. These grossly sectioned thin strips of tissues were then placed in nitroblue tetrazolium chloride (NBTC) stain overnight for viability staining.^{11,12} The remaining exposed tissue was embedded and submitted for frozen-section histologic processing and staining.

A digital single-lens reflex camera (Nikon D-70; Nikon USA, Melville, NY) was used for high-resolution photographs of IUS-exposed areas. Standardized conditions for distance and lighting were used for photography. Photographs were taken of the left and right side profiles of the face before and after IUS exposure (Figure 2). Digital photographs were also taken of the gross tissue sections after they had been stained with NBTC.

HISTOLOGIC ANALYSIS

Unfixed cadaveric tissue was used to more readily approximate human facial skin and to allow for evaluation in collagen by the NBTC viability stain.¹² When frozen tissue sections are stained, the reduction of nitroblue tetrazolium chloride (a redox indicator) by nicotinamide adenine dinucleotide (NADH) diaphorase produces an intense blue cytoplasmic pigment. The activity of nicotinamide adenine dinucleotide diaphorase has been shown to decrease immediately on cell death. Therefore, blue staining of cells on frozen sections using NBTC confirms viability, and the absence of blue staining is indicative of an

area of coagulative necrosis.¹³ We also performed routine hematoxylin-eosin regressive staining, which has also been used previously to demonstrate thermal denaturation of collagen for laser hair removal and ablative resurfacing.¹⁴ Both of these staining methods allow for accurate determination of the location and extent of the TIZs.

IMAGE ANALYSIS

Using image processing software (NIH ImageJ, available at <http://rsbweb.nih.gov/ij/>), postexposure digital photographs were compared with pretreatment images. The length of each horizontal and vertical line of the grids was then measured, recorded, and compared. The magnitude of thermal-induced immediate contraction was calculated by subtracting the postexposure distance from the preexposure distance, and then this number was divided by the preexposure distance and expressed as a percentage. Thermal-induced immediate contraction was compared parallel and perpendicular to the line of treatments to determine the maximum vector of collagen contraction. Depth and dimensions of TIZs were evaluated using digital photographs of gross tissue strips after NBTC staining.

RESULTS

A total of 202 IUS exposure lines (10 IUS pulses per line) and 2020 individual IUS pulses were delivered to the 6 cadaveric heads. After each exposure line, no noticeable surface changes were seen using either handpiece. Source conditions were varied across a range of 0.5 to 8.0 J for both handpieces. Viability staining (NBTC) identified le-

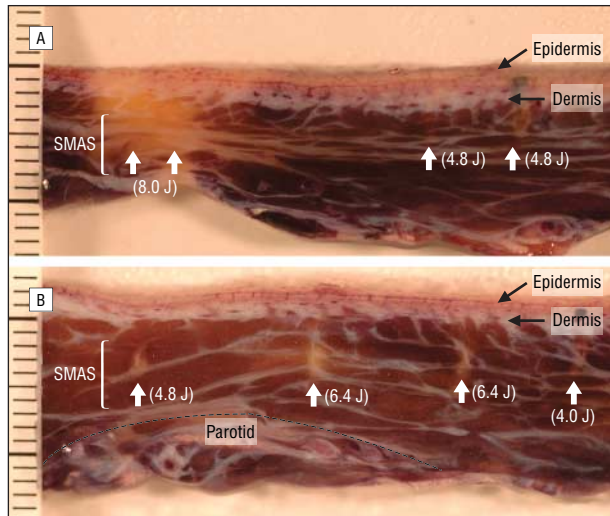


Figure 3. Zones of thermal injury: right preauricular area. Gross nitroblue tetrazolium chloride-stained sections of preauricular tissue after a set of intense ultrasound exposures using the 4.4-MHz/4.5-mm handpiece and 4.8 to 8.0 J of energy (A) and 4.0 to 6.4 J of energy (B). Arrows indicate thermal injury zones; SMAS, superficial musculoaponeurotic system. Scale indicates 1 mm per division.

sions on gross strips of cadaveric tissue as a lack of blue staining and pale color of the TIZs. Frozen-section histologic analysis of the same tissues also demonstrated the TIZs by lack of blue staining and morphologic evidence of thermal-induced coagulative necrosis, such as thickening of collagen fiber bundles. Thermal injury zone locations and dimensions were observed to be related to particular source conditions, such as energy and focal depth in tissue for a particular handpiece.

QUALITATIVE ANALYSIS OF TIZs

Visual analysis of the digital images of grossly sectioned strips of cadaveric tissues confirmed a dose-response relationship between energy and TIZ size. In the preauricular region, energy was varied between 3.2 and 8.0 J using the 4.4-MHz handpiece, and a dose-response effect of thermal modification was observed. Discrete cigar-shaped lesions can be seen in the SMAS layer without damage to surrounding tissues above or below (**Figure 3**). In this figure, small TIZs are easily identified at the lowest energy level of 4.0 J (**Figure 3B**). As the source energy is increased to 4.8 and then 6.4 J, the lesions become larger and more elongated. Further increases in energy lead to overtreatment as energy is increased to 8.0 J (**Figure 3A**). In this area in **Figure 3A**, 2 IUS exposure lines at an energy setting of 8.0 J are placed adjacent to one another. One can easily see the thermal damage extending proximally toward the source to involve the dermis and epidermis. No gross thermal lesions were seen at energy levels below 4.0 J (additional gross tissue strips from the same location not displayed in **Figure 3**). However, regressive hematoxylin-eosin-stained histologic slides of areas exposed to 3.2 J of energy confirmed the well-demarcated TIZs as evidenced by deep purple staining and thickening of the collagen bundles (**Figure 4**).

In the forehead region, when IUS exposures were delivered using the 4.4-MHz handpiece at similar energies

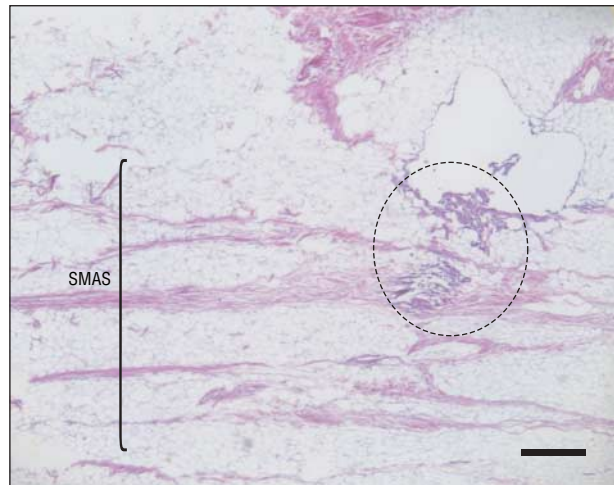


Figure 4. Histologic analysis of tissue taken from the right preauricular area. A discrete, intensely eosinophilic lesion (dotted circle) is seen in the superficial musculoaponeurotic system (SMAS) layer in this histologic section (regressive hematoxylin-eosin staining, original magnification $\times 20$; 4.4 MHz/4.5 mm; 3.2 J). Scale bar indicates 0.5 mm.

(2.3-6.1 J), overtreatment occurred at lower energy levels. At 3.8 J, the TIZs can be seen propagating superficially toward the dermis (**Figure 5**). As energy levels were increased further, the TIZs became thicker (**Figure 5A**). Conversely, when the energy settings were decreased, the TIZs became more slender (**Figure 5B**). This dose-response pattern could be observed in all of the NBTC-stained gross sections of tissues from all facial regions but was much more apparent in the forehead region. At the highest energy level of 6.1 J, NBTC histologic analysis revealed a lesion that extended from the mid dermis down through the subcutaneous fat to the level of the SMAS (**Figure 6**). In the middle dermis, thickening of collagen fibers is seen, with a loss of blue staining in the subdermis and SMAS that easily demarcates the lesion. The basement membrane revealed a cleft that separated the epidermis from the dermis (**Figure 6**).

In **Figure 7**, multiple TIZs can be seen discretely in the SMAS. In this region of the temple, a high-density line pattern was created using the 4.4-MHz handpiece. In this high-density pattern, multiple consecutive parallel exposure lines were delivered at the same unique power setting such that an array of densely spaced TIZs were deposited per unit volume of tissue. Relatively lower energy levels (3.0 J) compared with the cheek area were required to produce these well-defined lesions. In this gross tissue section, excellent consistency is demonstrated regarding TIZ depth and dimension. The NBTC-stained histologic analysis confirmed the successful targeting of the SMAS layer and the consistency of the closely spaced TIZ (**Figure 8**).

Intense ultrasound exposures using the higher-frequency 7.5-MHz handpiece with a 4.5-mm focal depth in tissue required much lower energy levels to create TIZs. Also, a much narrower window existed between creating discrete lesions in the SMAS and overtreatment. In **Figure 9**, we see a thin, well-demarcated lesion at 2.2 J; increasing the energy levels quickly results in over-

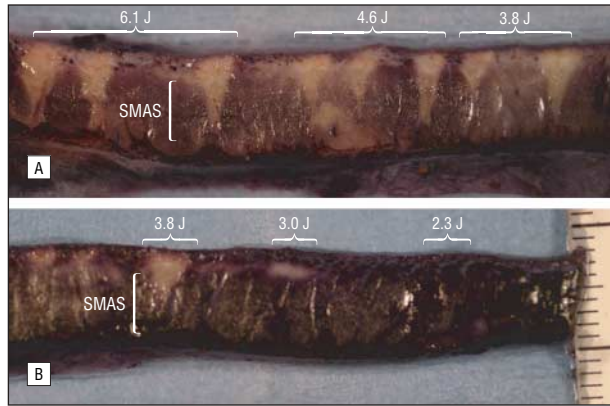


Figure 5. Zones of thermal injury: forehead area. Gross nitroblue tetrazolium chloride-stained sections of forehead tissue after a set of intense ultrasound exposures using the 4.4-MHz/4.5-mm handpiece and 3.8 to 6.1 J of energy (A) and 2.3 to 3.8 J of energy (B). SMAS indicates superficial musculoaponeurotic system. Scale indicates 1 mm per division.

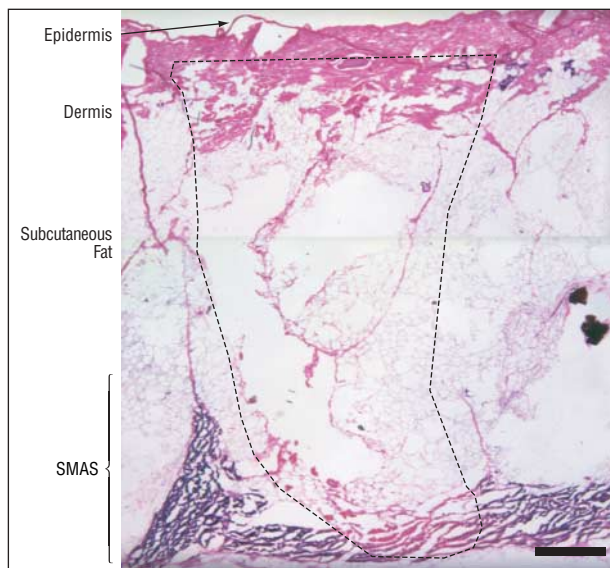


Figure 6. Nitroblue tetrazolium chloride histologic analysis: forehead area. Two photomicrographs were merged together to view a thermal injury zone (dotted line) extending from the mid dermis to the superficial musculoaponeurotic system (SMAS) layer (4.4 MHz/4.5 mm, 6.1 J, original magnification $\times 20$). Scale bar indicates 0.5 mm.

treated regions, as the 3.3 and 4.4 J exposure lines create lesions that approach the skin epidermis (tadpole phenomenon).⁹ At an energy exposure level of 1.6 J no gross lesion was produced; however, on NBTC histologic analysis, a discrete lesion was seen in the SMAS and connective tissue septae (**Figure 10**).

QUANTITATIVE ANALYSIS OF TIZS

Measurements were performed to quantify TIZ dimensions and depth of penetration in tissues as source energy settings were varied. Analysis of the digital images of grossly sectioned strips of cadaveric tissues after exposure using the 4.4-MHz handpiece confirmed a dose-response relationship (**Figure 11**). Figure 11A shows that TIZs at all energy levels were usually 0.5 mm below the tissue surface (top) and penetrated, on average, 5 mm deep into tissues (bottom). This corresponded closely to

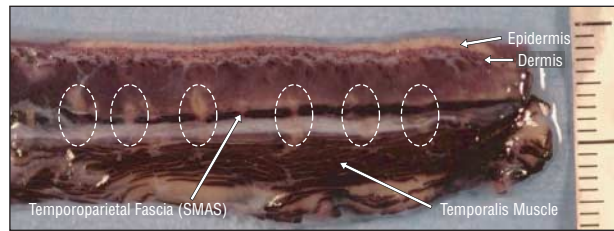


Figure 7. High-density line pattern of intense ultrasound exposures: left temporal area. The line of exposures is confined to the superficial musculoaponeurotic system (SMAS) layer (4.4 MHz/4.5 mm, 3.0 J). Dotted circles indicate thermal injury zones. Scale indicates 1 mm per division.

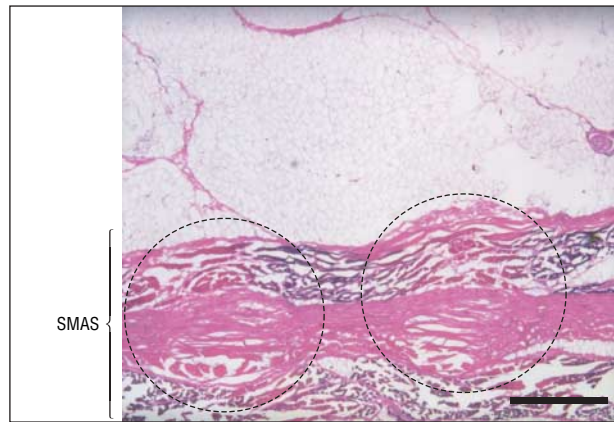


Figure 8. Nitroblue tetrazolium chloride histologic analysis: left temporal area. Two separate thermal injury zones (dotted circles) can be seen confined to the superficial musculoaponeurotic system (SMAS) layer (4.4 MHz/4.5 mm, 3.0 J, original magnification $\times 40$). Scale bar indicates 0.5 mm.

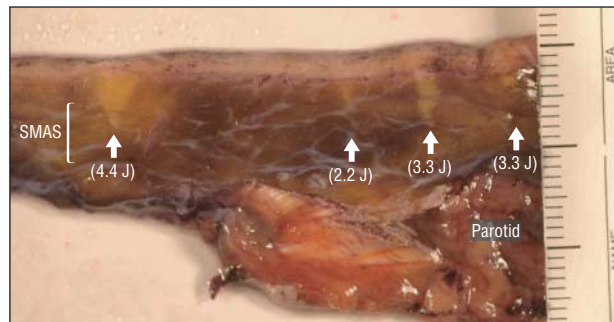


Figure 9. Zones of thermal injury: right cheek area. Gross nitroblue tetrazolium chloride-stained section of the cheek after a set of intense ultrasound exposures (7.5 MHz/4.5 mm, 2.2-4.4 J). Arrows indicate thermal injury zones; SMAS, superficial musculoaponeurotic system. Scale indicates 1 mm per division.

the preset focal depth of the 4.4-MHz handpiece (ie, 4.5 mm). A dose-response effect could be observed: as energy levels were increased from 3.8 to 8.0 J, TIZ dimensions increased proportionally (Figure 11B).

Using the 7.5-MHz handpiece, as energy levels were increased, the TIZs were close to the tissue surface (**Figure 12A**), which is what could be appreciated visually on the NBTC-stained gross cadaveric sections (Figure 9). Depth of penetration in tissue was variable but averaged 5.25 mm, which corresponded to the preset focal depth of the 7.5-MHz handpiece (4.5 mm) (Figure 12A). Analysis of the lesion size created (area in square millimeters) showed a close dose-response rela-

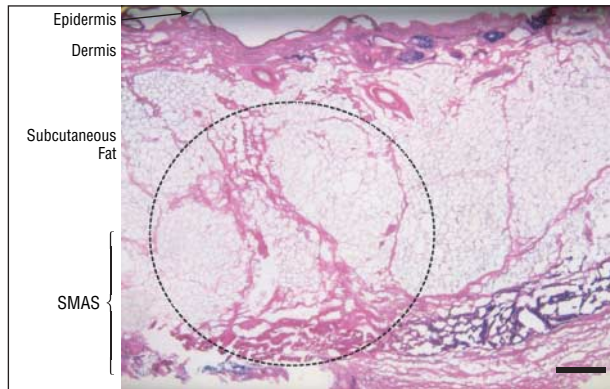


Figure 10. Nitroblue tetrazolium chloride histologic analysis: right forehead area. A well-defined thermal injury zone (dotted circle) is seen involving the superficial musculoaponeurotic system (SMAS) and overlying connective tissue septae. No gross lesion was identified in the tissue at this energy level (original magnification $\times 20$). Scale bar indicates 0.5 mm.

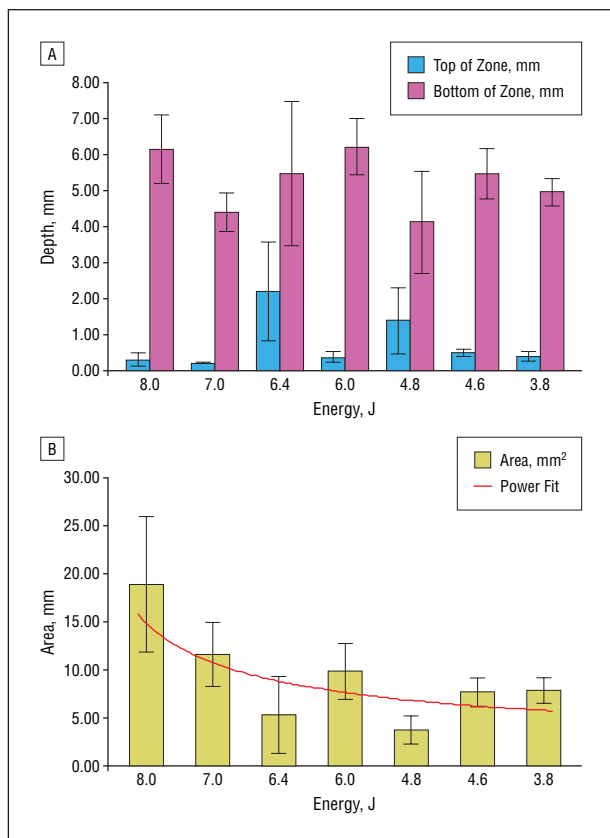


Figure 11. The dose response of the 4.4-MHz handpiece. A, Mean depth of lesions relative to the surface of the tissues. B, Mean changes in the dimensions of the lesion with decreasing energy levels. Error bars represent SD.

tionship: as the energy was increased, the TIZs became larger (Figure 12B).

THERMAL-INDUCED IMMEDIATE COLLAGEN CONTRACTION

Treated facial regions were observed to have small but reproducible degrees of collagen contraction. In general, the greater the energy levels delivered to tissues, the greater

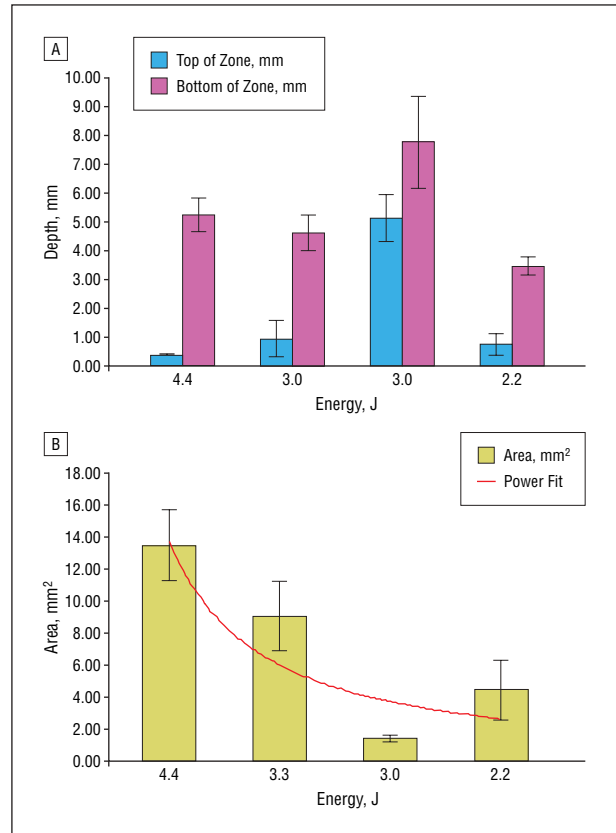


Figure 12. The dose response of the 7.5-MHz handpiece. A, Mean depth of lesions relative to the surface of the tissues. B, Mean changes in the dimensions of the lesion with decreasing energy levels. Error bars represent SD.

was the percentage contraction. In **Figure 13A**, we see that as the energy is increased from 3.1 to 6.7 J in these single-line exposures, the shrinkage increases. However, when multiple ($n=20$) IUS exposure lines are delivered, even at a much lower energy level (1.3 J), the shrinkage increases dramatically. As seen in the specimens, the high-density line pattern of exposure produces a greater number of TIZs per unit volume of soft tissue. When facial areas with a high-density line pattern were analyzed, the greatest degree of shrinkage occurred in the horizontal dimension, which was along the same axis as the greatest number of IUS exposures delivered (Figure 13B).

COMMENT

In this article, we introduce a novel technology with the potential for use in facial rejuvenation. We demonstrated that IUS is capable of creating zones of thermal injury (or areas of coagulative necrosis from heat) in the SMAS in human cadaveric soft tissues. These lesions are targeted, predictable, and reproducible in terms of depth, size, and shape based on handpiece frequency and source conditions (power, exposure time, and energy). Within the source conditions used in this study, the epidermis was spared even with increasing energy levels. Structures deep to the SMAS also were spared.

It is well established that IUS fields directed in soft tissue can produce ablation resulting primarily from thermal mechanisms.⁹ The energy from the ultrasound beam

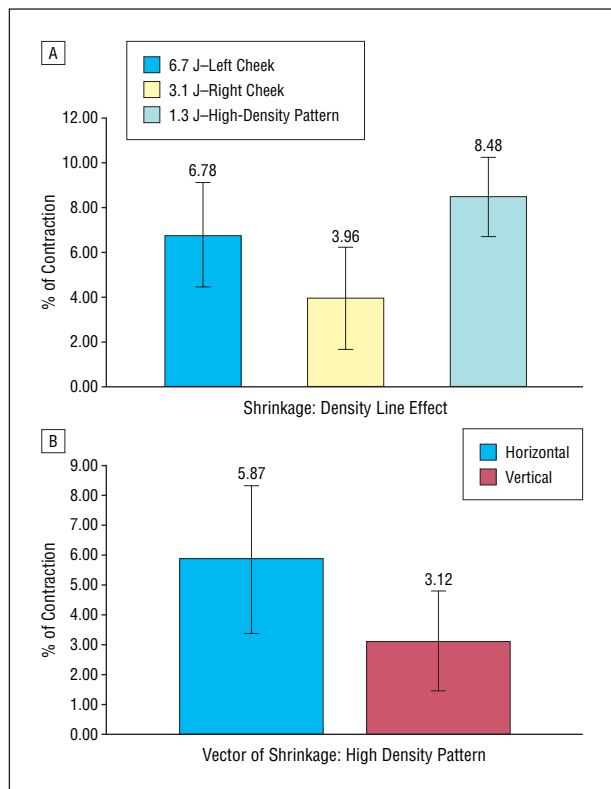


Figure 13. Thermal-induced immediate collagen contraction. A, As you increase the number of thermal injury zones per unit volume, you dramatically increase the amount of contraction (6.7 J, n=6; 3.1 J, n=6; and 1.3 J, n=20). B, In areas where a high-density line pattern was delivered, most shrinkage occurs along the horizontal direction, which was the same direction as the intense ultrasound exposures were delivered (n=65 per bar). Error bars represent SD.

is absorbed in the soft tissue and is converted primarily into heat. The increased temperature, in turn, results in distinct areas of coagulative necrosis of the tissue. In the case of skin tissue, the collagen is denatured (melted), and it loses its organized structure. This tissue response (thermal ablation) achieved by an IUS field is similar to that from other energy-based devices used in the cosmetic arena, such as lasers, RF, and combination laser-RF devices.⁶ However, in contrast to the other known energy-based devices used for cosmetic applications, the IUS field is sharply focused; thereby, most of the energy is deposited in the form of heat in the focal zone of the beam, leaving the surrounding regions unaffected. With RF delivery, thermal imaging has revealed that this energy is much more diffuse and tends to affect the dermis and travel along connective tissue septae in the subdermis.¹⁵

It has been demonstrated in this experiment that it is possible to create well-circumscribed TIZs selectively in the SMAS. No surface changes were noted on the cadaveric skin after exposure, and qualitative views of grossly stained tissue strips and histologic slides revealed no epidermal disruption. However, some overtreated areas revealed a characteristic cleft of the basal layer that is also seen immediately after laser therapy.¹⁶ Because this cleft was detected in untreated areas on histologic analysis, we believe that this may be a processing artifact.

The IUS system has been shown to produce a precise and reproducible line of lesions in tissues at a depth that

corresponds well to that handpiece's given fixed focal depth in tissue. The depth measurements of the TIZs were, on average, slightly deeper than the 4.5-mm focus. However, this may be the result of tissue swelling after immersion of the gross tissue strips in the NBTC stain. The depth of soft tissue also can affect lesion geometry. For example, in the preauricular region the soft tissue layer is comparatively thicker than other facial regions. As seen in Figure 3, IUS exposures using the 4.4-MHz handpiece produce discrete TIZs in the SMAS. However, in the forehead region the soft tissue layer is relatively thinner, and Figure 5 reveals overtreatment, or "tadpole formation" (a phenomenon that has been well documented for whole-organ ablation using IUS).¹⁷ This is likely due to reflected ultrasound waves from the periosteum and bone.

Although we demonstrated a small degree of immediate shrinkage after IUS exposure, this study is limited in the fact that the experimentation performed on cadaveric tissue is focused on evaluation of the immediate contraction induced by thermal denaturation of the collagen tissue. When tissue is heated to 65°C, there is a disruption of the intermolecular peptide bonds of the collagen triple helix (denaturation).⁷ As these bonds dissociate, the 3-dimensional structure unwinds, and an immediate collagen contraction ensues.

The use of ultrasound imaging to visualize the facial nerve and to direct therapies in the region, including the parotid gland, while avoiding the facial nerve has been successfully reported in Nd:YAG treatments of hemangiomas and vascular malformations of the head and neck.¹⁸ The subdermal delivery of energy in the face and neck has been reported with monopolar RF treatment (Thermage; Thermage Inc, Hayward, Calif) such as the non-surgical facelift procedure. However, these treatments do not produce focused lesions in a planned and targeted distribution, as demonstrated in this study. Furthermore, the simultaneous use of ultrasound for imaging and treatment of the SMAS has not been previously reported, to our knowledge.

This study suggests that IUS may have several characteristics that are particularly well suited to facial treatment. First, the technology leverages high-resolution ultrasound for imaging and treating the region in the same imaged field. The images generated provide a clear representation of the facial layers, including the skin, subcutaneous tissue, SMAS, and parotid. Second, we demonstrated that the lesion generated is highly selective regarding depth and size because these are directly related to the source frequency and the energy delivered. The handpieces used for this study are at a set frequency (7.5 or 4.4 MHz) and have a fixed focal depth in tissue (4.5 mm), limiting the nominal depth to which most of the energy is delivered in the tissue to approximately 5 mm. Higher energy levels produce lesions that are generally shallower and progress superficially. Lesions produced are consistent for a given region of facial tissue and source conditions, including the frequency and focal depth in tissue of a handpiece (which determines the depth of the lesion) and source energy of the pulse (which determines the size and shape of the lesion).

As a result, we can (1) image an appropriate area of interest and (2) deliver energy limited to a specific depth.

The mean \pm SD depths of the facial nerve in this area have been previously described in the literature¹⁹ as follows: main nerve trunk, 20.1 \pm 3.1 mm, and nerve exit from the parotid edge, 9.1 \pm 2.8 mm for temporal, 9.2 \pm 2.2 mm for zygomatic, 9.6 \pm 2.0 mm for buccal, and 10.6 \pm 2.7 mm for mandibular branches. These are all deep to the greatest depth produced in this study using the 2 handpiece frequencies and source configurations.

Histologic examination of IUS exposures demonstrated coagulative necrosis induced by thermal damage to the SMAS region while sparing the epidermis in a narrow range of energy levels. The characteristics of each of these histologic findings are similar to those of thermal ablation using other energy-based modalities, such as lasers and RF.¹⁵ The maximal area estimated for the zones of ablation achieved in this investigation are approximately 0.5 to 18 mm².

This study was limited by the fact that the human ambient body temperature is higher than the temperatures of the cadaveric tissue used in this experiment. Therefore, treatment levels in patients may require less energy to produce the same TIZs. Future clinical investigation in vivo is necessary to understand the effects of other factors, such as blood flow and immediate and delayed inflammatory reactions of the SMAS layer to TIZs.

In conclusion, we demonstrated in human cadaveric facial tissue that IUS energy can noninvasively image and selectively produce TIZs of reproducible location, size, and geometry in the SMAS layer. The ability to transcutaneously target the SMAS and to produce patterns of focused collagen denaturation to induce shrinkage has significant implications for aesthetic facial rejuvenation.

Accepted for Publication: October 1, 2006.

Correspondence: Richard E. Gliklich, MD, Division of Facial Plastic and Reconstructive Surgery, Massachusetts Eye and Ear Infirmary, 243 Charles St, Boston, MA 02114 (Richard_Gliklich@meei.harvard.edu).

Author Contributions: Drs Gliklich and White had full access to all of the data in the study and take responsibility for the integrity of the data and the accuracy of the data analysis. *Study concept and design:* White, Makin, Barthe, Slayton, and Gliklich. *Acquisition of data:* White, Makin, Barthe, Slayton, and Gliklich. *Analysis and interpretation of data:* White, Makin, Barthe, Slayton, and Gliklich. *Drafting of the manuscript:* White, Makin, Barthe, Slayton, and Gliklich. *Critical revision of the manuscript for important intellectual content:* White, Makin, Barthe, Slayton, and Gliklich. *Statistical analysis:* White, Makin, and Gliklich. *Obtained funding:* White and Gliklich. *Administrative, technical, and material support:* White, Makin, Barthe, Slayton, and Gliklich. *Study supervision:* White, Slayton, and Gliklich.

Financial Disclosure: Drs Makin, Slaton, and Barthe are Ulthera Inc stockholders and technology developers.

Funding/Support: This study was supported in part by funding from Ulthera Inc (Drs White and Gliklich).

Role of the Sponsor: This study was conducted in collaboration with Ulthera Inc, which had a role in the study design, data collection, data analysis, and writing of the manuscript.

REFERENCES

- Mitz V, Peyronie M. The superficial musculo-aponeurotic system (SMAS) in the parotid and cheek area. *Plast Reconstr Surg.* 1976;58:80-88.
- Ghassemi A, Prescher A, Riediger D, Axer H. Anatomy of the SMAS revisited. *Aesthetic Plast Surg.* 2003;27:258-264.
- Har-Shai Y, Sele E, Rubinstien I, Lindenbaum E, Mitz V, Hirshowitz B. Computerized morphometric quantification of elastin and collagen in SMAS and facial skin and the possible role of fat cells in SMAS viscoelastic properties. *Plast Reconstr Surg.* 1998;102:2466-2470.
- Thaller SR, Kim S, Patterson H, Wildman M, Daniloff A. The submuscular aponeurotic system (SMAS): a histologic and comparative anatomy evaluation. *Plast Reconstr Surg.* 1990;86:690-696.
- Har-Shai Y, Bodner SR, Egozy-Golan D, et al. Mechanical properties and microstructure of the superficial musculoaponeurotic system. *Plast Reconstr Surg.* 1996;98:59-70.
- Hruza GJ. Rejuvenating the aging face. *Arch Facial Plast Surg.* 2004;6:366-369.
- Ross EV, Naseef GS, McKinlay JR, et al. Comparison of carbon dioxide laser, erbium:YAG laser, dermabrasion, and dermatome: a study of thermal damage, wound contraction, and wound healing in a live pig model: implications for skin resurfacing. *J Am Acad Dermatol.* 2000;42:92-105.
- Kim KH, Geronemus RG. Nonablative laser and light therapies for skin rejuvenation. *Arch Facial Plast Surg.* 2004;6:398-409.
- Kennedy JE, ter Haar GR, Cranston D. High intensity focused ultrasound: surgery of the future? *Br J Radiol.* 2003;76:590-599.
- Mast TD, Makin IRS, Faidi W, Runk MM, Barthe PG, Slayton MH. Bulk ablation of soft tissue with intense ultrasound (IUS): modeling and ablation. *J Acoust Soc Am.* 2005;118:2715-2724.
- White WM, Makin IRS, Barthe PG, Slayton MH, Gliklich RE. Selective transcutaneous delivery of energy to facial subdermal tissues using the ultrasound therapy system [abstract]. *Lasers Surg Med.* 2006;suppl 18:113.
- Neumann RA, Knobler RM, Pieczkowski F, Gebhart W. Enzyme histochemical analysis of cell viability after argon laser-induced coagulation necrosis of the skin. *J Am Acad Dermatol.* 1991;25:991-998.
- Chung JH, Koh WS, Youn JI. Histological responses of port wine stains in brown skin after 578 nm copper vapor laser treatment. *Lasers Surg Med.* 1996;18:358-366.
- Majaron B, Kelly KM, Park HB, Verkruysse W, Nelson SJ. Er:YAG laser skin resurfacing using repetitive long-pulse exposure and cryogen spray cooling. I: histological study. *Lasers Surg Med.* 2001;28:121-130.
- Abraham MT, Ross EV. Current concepts in nonablative radiofrequency rejuvenation of the lower face and neck. *Facial Plast Surg.* 2005;21:65-73.
- Manstein D, Herron GS, Sink RK, Tanner H, Anderson RR. Fractional photothermolysis: a new concept for cutaneous remodeling using microscopic patterns of thermal injury. *Lasers Surg Med.* 2004;34:426-438.
- Meaney PM, Cahill MD, ter Haar GR, Cranston D. The intensity dependence of lesion position shift during focused ultrasound surgery. *Ultrasound Med Biol.* 2000;26:441-450.
- Werner JA, Lippert BM, Gottschlich S, et al. Ultrasound-guided interstitial Nd:YAG laser treatment of voluminous hemangiomas and vascular malformations in 92 patients. *Laryngoscope.* 1998;108:463-470.
- Rudolph R. Depth of the facial nerve in face lift dissections. *Plast Reconstr Surg.* 1990;85:537-544.